Nanomolar Pulse Dipolar EPR Spectroscopy in Proteins; the Cu^{II}- Cu^{II} and Nitroxide-Nitroxide Cases.

*Katrin Ackermann, Joshua L. Wort and Bela E. Bode**

EaStChem School of Chemistry, Biomedical Sciences Research Complex, and Centre of Magnetic Resonance, University of St Andrews, North Haugh, St Andrews, KY16 9ST, Scotland

Corresponding Author

*beb2@st-andrews.ac.uk

ABSTRACT. The study of ever more complex biomolecular assemblies implicated in human health and disease is facilitated by a suite of complementary biophysical methods. Pulse Dipolar Electron Paramagnetic Resonance (PDEPR) spectroscopy is a powerful tool that provides highly precise geometric constraints in frozen solution, however the drive towards PDEPR at physiologically relevant sub-µM concentrations is limited by the currently achievable concentration sensitivity. Recently, PDEPR using a combination of nitroxide and Cu^{II} based spin labels allowed measuring 500 nM concentration of a model protein. Using commercial instrumentation and spin labels we demonstrate Cu^{II}-Cu^{II} and nitroxide-nitroxide PDEPR measurements at protein concentrations more than an order of magnitude below previous examples reaching 500 and 100 nM, respectively. These results demonstrate the general feasibility of sub-µM PDEPR measurements at short to intermediate distances (~1.5 - 3.5 nm), and are of particular relevance for applications where the achievable concentration is limiting.

TOC GRAPHICS

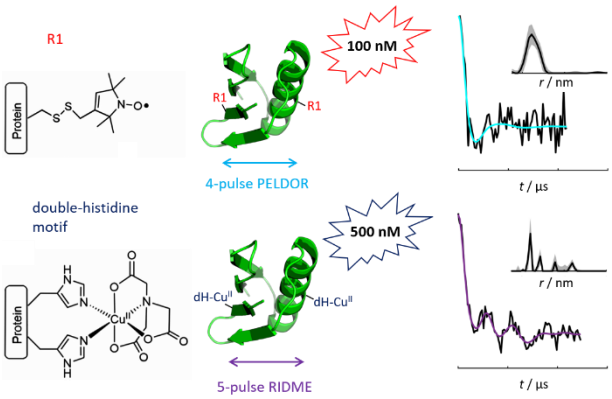

KEYWORDS EPR spectroscopy, Structural biology, PELDOR/DEER, RIDME, double-histidine motif.

The study of increasingly complex biomolecular assemblies and their interactions with the cellular environment has driven interest towards holistic structural characterization under conditions with high biological validity. Pulse dipolar EPR (PDEPR) is a powerful tool for such characterization, and complements X-ray crystallography, NMR, Förster resonance energy transfer (FRET), and cryo-EM data by providing solution-state distance constraints in systems of virtually unlimited size and complexity.[1-9] Due to these characteristics, PDEPR is also an emerging technique for conformational studies of protein and nucleic acid complexes in cellulo.[10-16] However, physiological concentrations are often in the sub-μM regime. In combination with low numbers of cells within samples, the challenge is to achieve sufficient absolute sensitivity. Analyzing a representative sample of 61 recent applications of nitroxide-nitroxide pulsed electron-electron double resonance (PELDOR)[17-18] measurements using the 4-pulse double electron-electron resonance (DEER)[19-20] sequence reveals the use of spin concentrations between 5 and 400 μM (median 100 μM, mean 116 ± 90 μM, see SI) demonstrating the current state of the art. While measurements down to 1 μM should be feasible we could not identify a single published example. Recently, Cu^{II}-nitroxide 5-pulse relaxation induced dipolar modulation enhancement (RIDME)[21-22] measurements at 500 nM concentration in a protein *in vitro* allowed not only precise distance measurements but also determination of the binding affinity.[23] Thereby, demonstrating the high-affinity of genetically encoded double-histidine motifs to Cu^{II} ions,[24-25] and their suitability as labelling sites for low concentration studies.[26]

Herein, we approach practical concentration limits associated with PDEPR experiments and found Cu^{II}-Cu^{II} RIDME measurements and nitroxide-nitroxide PELDOR measurements feasible at 500 nM and 100 nM protein concentration, respectively (corresponding to spin concentrations

of 1.6 µM and 200 nM, respectively). Importantly, these measurements were performed in a commercial non-broadband Q-band spectrometer, using well-established spin labels, methanethiosulfonate (MTSL)[27-28] and Cu^{II}-nitrilotriacetic acid (Cu^{II}-NTA)[25] (figure 1). To our knowledge this is the first demonstration of sub-µM Cu^{II}-Cu^{II} and nitroxide-nitroxide PDEPR measurements in a biological system.

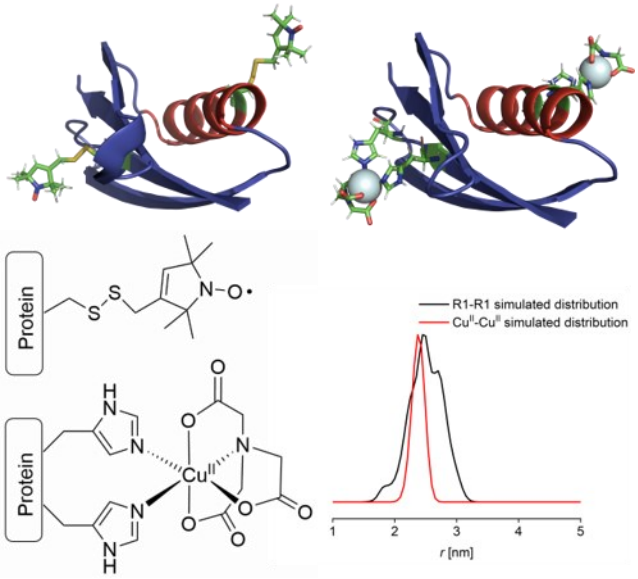

Figure 1. GB1 constructs, spin label structures and simulated distance distributions. Top: Cartoon representations of GB1 constructs I6R1/K28R1 (left) and I6H/N8H/K28H/Q32H (right), with spin labels shown in stick representation. Bottom: Chemical structures of R1 nitroxide and double histidine Cu^{II}-NTA spin labels (left). Corresponding simulated distance distribution (right) for each construct, shown in black and red, respectively.

Commercial instruments have been used successfully for PELDOR measurements at low µM concentration.[29] Concentration sensitivity has been demonstrated to further improve in homebuilt high-power resonator-free spectrometers[30-31] or by implementation of arbitrary waveform generators (AWGs) and shaped pulses that yield higher spin inversion efficiencies.[32-36]

Additionally, novel pulse sequences have shown to enhance measurement sensitivity.[37-40] Trityl-based radicals[41-43] with exquisitely narrow spectral linewidths have been measured at 45 nM protein (90 nM spin) concentration[41] employing the single-frequency double quantum coherence (DQC)[44] experiment. This is a remarkable achievement owed to bespoke narrow line spin labels allowing use of a single-frequency technique. It is not currently established where the limits are for the most common 4-pulse DEER method applied to the most popular nitroxide labels, nor for the emerging use of RIDME on Cu^{II}-labels.

In the current study, *Streptococcus sp*. Group G protein G, B1 domain (GB1) constructs (I6R1/K28R1 and I6H/N8H/K28H/Q32H) were used as biological model systems (figure 1). GB1 has been used extensively in previous EPR methodology studies.[23-26, 45-48] We have shown previously that nitroxide-detected Cu^{II}-nitroxide and Cu^{II}-Cu^{II} RIDME are similar in sensitivity and roughly two orders of magnitude more sensitive than Cu^{II}-Cu^{II} PELDOR when limited to rectangular pulses.[23] Here, we endeavored to test the sensitivity of the most widespread pulse dipolar EPR methodology, nitroxide-nitroxide PELDOR.[49] Therefore Cu^{II}-Cu^{II} RIDME and nitroxide-nitroxide PELDOR were measured at 500 nM concentration for a direct comparison of experiment sensitivity (figure 2).

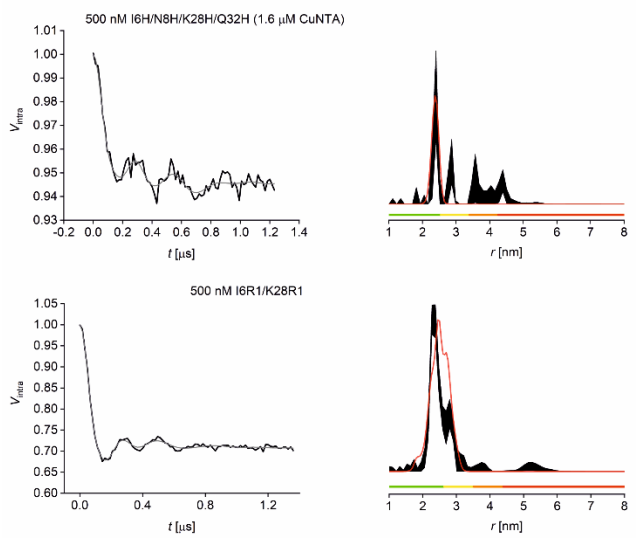

Figure 2. 500 nM GB1 Cu^{II}-Cu^{II} RIDME and nitroxide-nitroxide PELDOR Q-band data at 30 and 50 K, respectively. Top: RIDME data for 500 nM GB1 tetra-histidine with 1.6 µM Cu^{II}-NTA added. Bottom: PELDOR data for 500 nM GB1 I6R1/K28R1. Left: Background-corrected data (black) and fit (grey). Right: Corresponding distance distributions given as 95% confidence intervals (± 2σ) with 50% noise added for error estimation during statistical analysis; simulated distance distributions are shown in red. Color bars represent reliability ranges (green: shape reliable; yellow: mean and width reliable; orange: mean reliable; red: no quantification possible).

The optimum temperatures with respect to sensitivity were found to be 30 K and 50 K, respectively (see SI). As RIDME is a single frequency technique, it can be performed with all pulses coinciding with the resonance frequency of the resonator and thus benefits in sensitivity compared to double frequency techniques, such as the 4-pulse DEER sequence where detection is generally performed off-resonance. This sensitivity gain in dependence of the cavity quality factor being adjusted to meet the required bandwidth could be quantified as approximately a factor 2 (see SI). Furthermore, the influence of instantaneous diffusion (that occurs when dephasing is induced by dipolarly coupled spins being inverted by detection pulses reducing the

detected echo) was shown to be negligible in the I6R1/K28R1 construct at both 500 nM and 25 μM concentrations (see SI).

For the Cu^{II}-Cu^{II} RIDME data shown in figure 2, only the distance peak at ~2.5 nm was shown to be stable upon data validation. Additional measurements at 500 μM protein concentration suggested the distribution peaks above 2.5 nm were artefacts, insignificant in the 95% confidence interval (see SI). This indicated that measurements at 500 nM tetra-histidine protein concentration likely approached the lower concentration limit for Cu^{II}-Cu^{II} RIDME in our hands. It should be noted that the poor modulation depth (5.5%) is a result of the limiting affinity of Cu^{II}-NTA for the β-sheet double histidine motif.[23] Pulse dipolar EPR methods allow precise determination of binding affinities from PELDOR[50-52] and RIDME[53] data. The observed modulation depth is consistent with predictions using binding affinities previously derived from Cu^{II}-nitroxide RIDME pseudo-titration[23] and extrapolated ITC data (see SI). Conversely, for the nitroxide-nitroxide PELDOR data the bimodal distribution shown in figure 2 was recapitulated in additional measurements at 25 μM I6R1/K28R1 protein concentration (see SI). This suggested that measurements at 500 nM protein concentration were not yet testing the lower concentration limit for nitroxide-nitroxide PELDOR. To test this hypothesis, nitroxide-nitroxide PELDOR was also measured at 100 nM protein (200 nM spin) concentration (figure 3).

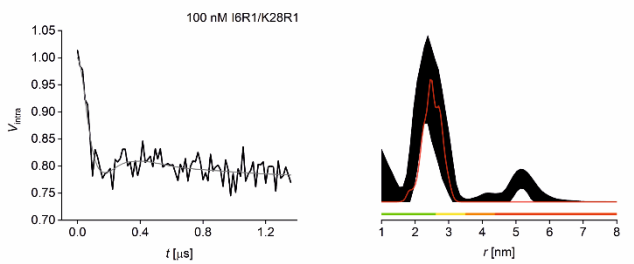

Figure 3. 100 nM GB1 Q-band PELDOR data at 50K. Left: Background-corrected PELDOR data (black) and fit (grey) for 100 nM I6R1/K28R1 GB1. Right: Corresponding distance distribution given as 95% confidence intervals (± 2σ) with 50% noise added for error estimation during statistical analysis; simulated distance distributions are shown in red. Color bars represent reliability ranges (green: shape reliable; yellow: mean and width reliable; orange: mean reliable; red: no quantification possible).

The nitroxide-nitroxide PELDOR data shown in figure 3, measured with the same dipolar evolution time for comparison, indicate that at 100 nM the retrieved experimental distribution is no longer bimodal, however the mean distance is still retrieved as the only significant peak following data validation. Nevertheless, the relatively poor signal-to-noise ratio mandates a regularization parameter that does not allow resolving both distance populations (SI). This loss in resolution has been confirmed using other processing approaches (see SI for details). This experiment thus highlights the dependence of distance resolution on achievable signal-to-noise and thus, on spin concentration. Together, this suggests that 100 nM approaches the minimum concentration achievable for reliable determination of the mean distance from nitroxide-nitroxide PELDOR under our conditions; it is already beyond a reliable determination of the distance distribution shape. Sensitivity analysis shows that measurement of I6R1/K28R1 at 100 nM is a factor ~15 noisier than measurement at 500 nM, rather than the factor 5 expected from the

concentration difference. The additional factor 3 can be considered a penalty for the challenging measurement optimization at these very low concentrations (see SI).

Comparing the relative sensitivities of nitroxide-nitroxide PELDOR and Cu^{II}-Cu^{II} RIDME reveals the former to be approximately 10-fold more sensitive (see SI). The 3 main factors contributing to the relative sensitivity are echo amplitude (i.e., signal-to-noise), modulation depth, and averaging rate. For Cu^{II}-Cu^{II} RIDME the smaller signal is largely compensated by the faster averaging. However, the modulation depth is a limiting factor for sensitivity. This is to be expected for a non-covalent spin-label with dissociation constants in the high nM (α-helix) and low μM (β-sheet) regime. Overcoming the low modulation depth will make sensitivity of Cu^{II}-Cu^{II} RIDME competitive. Simulation of a tetra-histidine construct containing a pair of α-helical binding sites reveals modulation depths > 12% for Cu^{II}-Cu^{II} RIDME under otherwise identical conditions (see SI). Possible strategies to further improve modulation depths include insertion of an artificial amino-acid bearing a covalent Cu^{II} centre to overcome the limiting equilibrium constants,[54] or measuring nitroxide detected Cu^{II}-nitroxide RIDME in excess Cu^{II} chelate spin label. This will shift the binding equilibrium into saturation of the binding site and achieve modulation depths approaching 50%, independent of protein concentration.

Comparing nitroxide-nitroxide PELDOR with available Cu^{II}-nitroxide RIDME data[23] suggests the latter to be an additional factor ~1.5 more sensitive potentially allowing measurements even below 100 nM protein concentration (see SI). Additionally, RIDME measurements may be less prone to the optimization penalty found for 4-pulse DEER at 100 nM as the single-frequency method will need fewer parameters to be set. These findings showcase that in favorable circumstances superb concentration sensitivities are achievable using commercial

instrumentation and spin labels. In the case of the widely applied nitroxide-nitroxide 4-pulse DEER experiment, concentration sensitivities orders of magnitude greater than routinely applied (≥10 μM) are possible using rectangular pulses at Q-band frequencies. Additionally, Cu^{II}-Cu^{II} RIDME measurements showcase that systems not amenable to conventional thiol-based covalent spin labelling are also accessible in the sub-μM concentration regime, when used in conjunction with double-histidine motifs. Concentrations realized here for Cu^{II}-Cu^{II} RIDME are more than an order of magnitude below published applications of the 5-pulse RIDME experiment on metal-metal spin systems (≥ 25 μM; see SI).

Nevertheless, at these low concentrations long distances or more complex distance distributions will be a challenge for both, nitroxide-nitroxide DEER and Cu^{II}-Cu^{II} RIDME experiments. The presence of conformational flexibility or two (or more) conformational states will result in broad or multimodal distance distributions, respectively. The superposition of frequencies will lead to less pronounced oscillations and a larger ambiguity in the distance analysis.[55] While the distance distribution mean and width were recoverable from the 100 nM GB1 sample the bimodal distribution was only resolved in the 500 nM sample. Long distances and highly resolved distance distributions require longer dipolar evolution times. In these cases, sensitivity enhancement is achievable by full deuteration of protein and matrix due to decreased echo dephasing (increased phase memory time T_M).[56-57] The benefit that can be realised from deuteration will strongly depend on the required trace lengths.

In conclusion, benchmarking the nanomolar sensitivity is truly promising as a pathway to novel applications and may facilitate study of systems previously thought to be beyond the scope of pulse EPR spectroscopy. Perhaps most importantly, our results emphasize that commercial instrumentation and standard labelling protocols already yield sufficient concentration sensitivity

for applications in the sub-μM regime. The imminent adoption of cryogenically cooled preamplifiers for EPR spectroscopy[58] heralds a further order of magnitude of sensitivity improvement. Embracing the opportunity to measure at concentrations two to three orders of magnitude below past practice will bring new science into reach that is currently sample limited in either concentration or absolute amount.

ASSOCIATED CONTENT

Supporting Information. The following files are available free of charge: Supporting information (PDF). Content: 1. Experimental procedures, 2. Temperature-dependent relaxation behaviour, 3. Additional RIDME data, 4. Additional PELDOR data, 5. Deep neural network processing and wavelet denoising, 6. Instantaneous diffusion, 7. Sensitivity considerations, 8. Literature search, 9. References.

Notes

The authors declare no competing financial interests.

ACKNOWLEDGMENT

We thank Dr Angeliki Giannoulis for insightful discussions. This research was funded, in whole or in part, by the Wellcome Trust (099149/Z/12/Z and 204821/Z/16/Z). BEB and KA acknowledge support by the Leverhulme Trust (RPG-2018–397). JLW is supported by the BBSRC DTP Eastbio. BEB acknowledges equipment funding by BBSRC (BB/R013780/1).

REFERENCES

(1) Constantinescu-Aruxandei, D.; Petrovic-Stojanovska, B.; Schiemann, O.; Naismith, J. H.; White, M. F. Taking a Molecular Motor for a Spin: Helicase Mechanism Studied by Spin

Labeling and PELDOR. *Nucleic Acids Res.* **2016,** *44*, 954-968, https://di.org/10.1093/nar/gkv1373.

(2) Duss, O.; Michel, E.; Yulikov, M.; Schubert, M.; Jeschke, G.; Allain, F. H. T. Structural Basis of the Non-Coding RNA RsmZ Acting as a Protein Sponge. *Nature* **2014,** *509*, 588-592, https://doi.org/10.1038/nature13271.

(3) Ghosh, S.; Lawless, M. J.; Brubaker, H. J.; Singewald, K.; Kurpiewski, M. R.; Jen-Jacobson, L.; Saxena, S. Cu^{2+}-Based Distance Measurements by Pulsed EPR Provide Distance Constraints for DNA Backbone Conformations in Solution. *Nucleic Acids Res.* **2020,** *48*, e49-e49, https://doi.org/10.1093/nar/gkaa133.

(4) Hagelueken, G.; Ingledew, W. J.; Huang, H.; Petrovic-Stojanovska, B.; Whitfield, C.; ElMkami, H.; Schiemann, O.; Naismith, J. H. PELDOR Spectroscopy Distance Fingerprinting of the Octameric Outer-Membrane Protein Wza from *Escherichia coli*. *Angew. Chem. Int. Ed.* **2009,** *48*, 2904-2906, https://doi.org/10.1002/anie.200805758.

(5) Joseph, B.; Sikora, A.; Bordignon, E.; Jeschke, G.; Cafiso, D. S.; Prisner, T. F. Distance Measurement on an Endogenous Membrane Transporter in *E. coli* Cells and Native Membranes Using EPR Spectroscopy. *Angew. Chem. Int. Ed.* **2015,** *54*, 6196-6199, https://doi.org/10.1002/anie.201501086.

(6) Kapsalis, C.; Wang, B.; El Mkami, H.; Pitt, S. J.; Schnell, J. R.; Smith, T. K.; Lippiat, J. D.; Bode, B. E.; Pliotas, C. Allosteric Activation of an Ion Channel Triggered by Modification of Mechanosensitive Nano-Pockets. *Nat Commun* **2019,** *10*, 4619-4619, https://doi.org/10.1038/s41467-019-12591-x.

(7) Sameach, H.; Ghosh, S.; Gevorkyan-Airapetov, L.; Saxena, S.; Ruthstein, S. EPR Spectroscopy Detects Various Active State Conformations of the Transcriptional Regulator CueR. *Angew. Chem. Int. Ed.* **2019,** *58*, 3053-3056, https://doi.org/10.1002/anie.201810656.

(8) Schmidt, T.; Wälti, M. A.; Baber, J. L.; Hustedt, E. J.; Clore, G. M. Long Distance Measurements up to 160 Å in the GroEL Tetradecamer Using Q-Band DEER EPR Spectroscopy. *Angew. Chem. Int. Ed.* **2016,** *55*, 15905-15909, https://doi.org/10.1002/anie.201609617.

(9) Verhalen, B.; Dastvan, R.; Thangapandian, S.; Peskova, Y.; Koteiche, H. A.; Nakamoto, R. K.; Tajkhorshid, E.; McHaourab, H. S. Energy Transduction and Alternating Access of the Mammalian ABC Transporter P-Glycoprotein. *Nature* **2017,** *543*, 738-741, https://doi.org/10.1038/nature21414.

(10) Azarkh, M.; Bieber, A.; Qi, M.; Fischer, J. W. A.; Yulikov, M.; Godt, A.; Drescher, M. Gd(III)-Gd(III) Relaxation-Induced Dipolar Modulation Enhancement for In-Cell Electron Paramagnetic Resonance Distance Determination. *J. Phys. Chem. Lett.* **2019,** *10*, 1477-1481, https://doi.org/10.1021/acs.jpclett.9b00340.

(11) Igarashi, R.; Sakai, T.; Hara, H.; Tenno, T.; Tanaka, T.; Tochio, H.; Shirakawa, M. Distance Determination in Proteins inside *Xenopus laevis* Oocytes by Double Electron−Electron Resonance Experiments. *J. Am. Chem. Soc.* **2010,** *132*, 8228-8229, https://doi.org/10.1021/ja906104e.

(12) Jassoy, J. J.; Berndhäuser, A.; Duthie, F.; Kühn, S. P.; Hagelueken, G.; Schiemann, O. Versatile Trityl Spin Labels for Nanometer Distance Measurements on Biomolecules In Vitro and within Cells. *Angew. Chem. Int. Ed.* **2017,** *56*, 177-181, https://doi.org/10.1002/anie.201609085.

(13) Joseph, B.; Sikora, A.; Cafiso, D. S. Ligand Induced Conformational Changes of a Membrane Transporter in *E. coli* Cells Observed with DEER/PELDOR. *J. Am. Chem. Soc.* **2016,** *138*, 1844-1847, https://doi.org/10.1021/jacs.5b13382.

(14) Krstić, I.; Hänsel, R.; Romainczyk, O.; Engels, J. W.; Dötsch, V.; Prisner, T. F. Long-Range Distance Measurements on Nucleic Acids in Cells by Pulsed EPR Spectroscopy. *Angew. Chem. Int. Ed.* **2011,** *50*, 5070-5074, https://doi.org/10.1002/anie.201100886.

(15) Theillet, F.-X.; Binolfi, A.; Bekei, B.; Martorana, A.; Rose, H. M.; Stuiver, M.; Verzini, S.; Lorenz, D.; van Rossum, M.; Goldfarb, D.; Selenko, P. Structural Disorder of Monomeric α-Synuclein Persists in Mammalian Cells. *Nature* **2016,** *530*, 45-50, https://doi.org/10.1038/nature16531.

(16) Yang, Y.; Chen, S.-N.; Yang, F.; Li, X.-Y.; Feintuch, A.; Su, X.-C.; Goldfarb, D. In-Cell Destabilization of a Homodimeric Protein Complex Detected by DEER Spectroscopy. *Proc Natl Acad Sci U S A* **2020,** *117*, 20566-20575, https://doi.org/10.1073/pnas.2005779117.

(17) Milov, A. D.; Ponomarev, A. B.; Tsvetkov, Y. D. Electron-Electron Double Resonance in Electron Spin Echo: Model Biradical Systems and the Sensitized Photolysis of Decalin. *Chem. Phys. Lett.* **1984,** *110*, 67-72, https://doi.org/10.1016/0009-2614(84)80148-7.

(18) Milov, A. D.; Salikov, K. M.; Shirov, M. D. Application of ELDOR in Electron-Spin Echo for Paramagnetic Center Space Distribution in Solids. *Fiz. Tverd. Tela* **1981,** *23*, 975-982,

(19) Martin, R. E.; Pannier, M.; Diederich, F.; Gramlich, V.; Hubrich, M.; Spiess, H. W. Determination of End-to-End Distances in a Series of TEMPO Diradicals of up to 2.8 nm Length with a New Four-Pulse Double Electron Electron Resonance Experiment. *Angew. Chem. Int. Ed.*

1998, *37*, 2833-2837, https://doi.org/10.1002/(SICI)1521-3773(19981102)37:20<2833::AID-ANIE2833>3.0.CO;2-7.

(20) Pannier, M.; Veit, S.; Godt, A.; Jeschke, G.; Spiess, H. W. Dead-Time Free Measurement of Dipole-Dipole Interactions between Spins. *J. Magn. Reson.* **2000,** *142*, 331-340, https://doi.org/10.1006/jmre.1999.1944.

(21) Kulik, L. V.; Dzuba, S. A.; Grigoryev, I. A.; Tsvetkov, Y. D. Electron Dipole–Dipole Interaction in ESEEM of Nitroxide Biradicals. *Chem. Phys. Lett.* **2001,** *343*, 315-324, https://doi.org/10.1016/S0009-2614(01)00721-7.

(22) Milikisyants, S.; Scarpelli, F.; Finiguerra, M. G.; Ubbink, M.; Huber, M. A Pulsed EPR Method to Determine Distances Between Paramagnetic Centers with Strong Spectral Anisotropy and Radicals: The Dead-time Free RIDME Sequence. *J. Magn. Reson.* **2009,** *201*, 48-56, https://doi.org/10.1016/j.jmr.2009.08.008.

(23) Wort, J. L.; Ackermann, K.; Giannoulis, A.; Stewart, A. J.; Norman, D. G.; Bode, B. E. Sub-Micromolar Pulse Dipolar EPR Spectroscopy Reveals Increasing Cu^{II}-labelling of Double-Histidine Motifs with Lower Temperature. *Angew. Chem. Int. Ed.* **2019,** *58*, 11681-11685, https://doi.org/10.1002/anie.201904848.

(24) Cunningham, T. F.; Putterman, M. R.; Desai, A.; Horne, W. S.; Saxena, S. The Double-Histidine Cu^{2+}-Binding Motif: a Highly Rigid, Site-Specific Spin Probe for Electron Spin Resonance Distance Measurements. *Angew. Chem. Int. Ed.* **2015,** *54*, 6330-6334, https://doi.org/10.1002/anie.201501968.

(25) Ghosh, S.; Lawless, M. J.; Rule, G. S.; Saxena, S. The Cu^{2+}-Nitrilotriacetic Acid Complex Improves Loading of α-Helical Double Histidine Site for Precise Distance Measurements by Pulsed ESR. *J. Magn. Reson.* **2018,** *286*, 163-171, https://doi.org/10.1016/j.jmr.2017.12.005.

(26) Wort, J. L.; Arya, S.; Ackermann, K.; Stewart, A. J.; Bode, B. E. Pulse Dipolar EPR Reveals Double-Histidine Motif Cu^{II}–NTA Spin-Labeling Robustness against Competitor Ions. *J. Phys. Chem. Lett.* **2021,** *12*, 2815-2819, https://doi.org/10.1021/acs.jpclett.1c00211.

(27) Berliner, L. J.; Grunwald, J.; Hankovszky, H. O.; Hideg, K. A Novel Reversible Thiol-Specific Spin Label: Papain Active Site Labeling and Inhibition. *Anal. Biochem.* **1982,** *119*, 450-455, https://doi.org/10.1016/0003-2697(82)90612-1.

(28) Hubbell, W. L.; Altenbach, C. Investigation of Structure and Dynamics in Membrane Proteins Using Site-Directed Spin Labeling. *Current Opinion in Structural Biology* **1994,** *4*, 566-573, https://doi.org/10.1016/S0959-440X(94)90219-4.

(29) Babaylova, E. S.; Malygin, A. A.; Lomzov, A. A.; Pyshnyi, D. V.; Yulikov, M.; Jeschke, G.; Krumkacheva, O. A.; Fedin, M. V.; Karpova, G. G.; Bagryanskaya, E. G. Complementary-Addressed Site-Directed Spin Labeling of Long Natural RNAs. *Nucleic Acids Res.* **2016,** *44*, 7935-7943, https://doi.org/10.1093/nar/gkw516.

(30) Cruickshank, P. A. S.; Bolton, D. R.; Robertson, D. A.; Hunter, R. I.; Wylde, R. J.; Smith, G. M. A Kilowatt Pulsed 94 GHz Electron Paramagnetic Resonance Spectrometer with High Concentration Sensitivity, High Instantaneous Bandwidth, and Low Dead Time. *Rev. Sci. Instrum.* **2009,** *80*, 103102, https://doi.org/10.1063/1.3239402.

(31) Hofbauer, W.; Earle, K. A.; Dunnam, C. R.; Moscicki, J. K.; Freed, J. H. High-Power 95 GHz Pulsed Electron Spin Resonance Spectrometer. *Rev. Sci. Instrum.* **2004,** *75*, 1194-1208, https://doi.org/10.1063/1.1710700.

(32) Breitgoff, F. D.; Keller, K.; Qi, M.; Klose, D.; Yulikov, M.; Godt, A.; Jeschke, G. UWB DEER and RIDME Distance Measurements in Cu(II)-Cu(II) Spin Pairs. *J. Magn. Reson.* **2019,** *308*, 106560, https://doi.org/10.1016/j.jmr.2019.07.047.

(33) Doll, A.; Pribitzer, S.; Tschaggelar, R.; Jeschke, G. Adiabatic and Fast Passage Ultra-Wideband Inversion in Pulsed EPR. *J. Magn. Reson.* **2013,** *230*, 27-39, https://doi.org/10.1016/j.jmr.2013.01.002.

(34) Motion, C. L.; Cassidy, S. L.; Cruickshank, P. A. S.; Hunter, R. I.; Bolton, D. R.; El Mkami, H.; Van Doorslaer, S.; Lovett, J. E.; Smith, G. M. The use of Composite Pulses for Improving DEER Signal at 94GHz. *J. Magn. Reson.* **2017,** *278*, 122-133, https://doi.org/10.1016/j.jmr.2017.03.018.

(35) Spindler, P. E.; Glaser, S. J.; Skinner, T. E.; Prisner, T. F. Broadband Inversion PELDOR Spectroscopy with Partially Adiabatic Shaped Pulses. *Angew. Chem. Int. Ed.* **2013,** *52*, 3425-3429, https://doi.org/10.1002/anie.201207777.

(36) Spindler, P. E.; Zhang, Y.; Endeward, B.; Gershernzon, N.; Skinner, T. E.; Glaser, S. J.; Prisner, T. F. Shaped Optimal Control Pulses for Increased Excitation Bandwidth in EPR. *J. Magn. Reson.* **2012,** *218*, 49-58, https://doi.org/10.1016/j.jmr.2012.02.013.

(37) Bahrenberg, T.; Yang, Y.; Goldfarb, D.; Feintuch, A. rDEER: A Modified DEER Sequence for Distance Measurements Using Shaped Pulses. *Magnetochemistry* **2019,** *5*, https://doi.org/10.3390/magnetochemistry5010020.

(38) Borbat, P. P.; Georgieva, E. R.; Freed, J. H. Improved Sensitivity for Long-Distance Measurements in Biomolecules: Five-Pulse Double Electron–Electron Resonance. *J. Phys. Chem. Lett.* **2013,** *4*, 170-175, https://doi.org/10.1021/jz301788n.

(39) Doll, A.; Qi, M.; Pribitzer, S.; Wili, N.; Yulikov, M.; Godt, A.; Jeschke, G. Sensitivity Enhancement by Population Transfer in Gd(III) Spin Labels. *Phys. Chem. Chem. Phys.* **2015,** *17*, 7334-7344, https://doi.org/10.1039/C4CP05893C.

(40) Spindler, P. E.; Waclawska, I.; Endeward, B.; Plackmeyer, J.; Ziegler, C.; Prisner, T. F. Carr–Purcell Pulsed Electron Double Resonance with Shaped Inversion Pulses. *J. Phys. Chem. Lett.* **2015,** *6*, 4331-4335, https://doi.org/10.1021/acs.jpclett.5b01933.

(41) Fleck, N.; Heubach, C.; Hett, T.; Spicher, S.; Grimme, S.; Schiemann, O. Ox-SLIM: Synthesis of and Site-Specific Labelling with a Highly Hydrophilic Trityl Spin Label. *Chem. Eur. J.* **2021,** *27*, 5292-5297, https://doi.org/10.1002/chem.202100013.

(42) Reginsson, G. W.; Kunjir, N. C.; Sigurdsson, S. T.; Schiemann, O. Trityl Radicals: Spin Labels for Nanometer-Distance Measurements. *Chem. Eur. J.* **2012,** *18*, 13580-13584, https://doi.org/10.1002/chem.201203014.

(43) Yang, Z.; Liu, Y.; Borbat, P.; Zweier, J. L.; Freed, J. H.; Hubbell, W. L. Pulsed ESR Dipolar Spectroscopy for Distance Measurements in Immobilized Spin Labeled Proteins in Liquid Solution. *J. Am. Chem. Soc.* **2012,** *134*, 9950-9952, 10.1021/ja303791p.

(44) Borbat, P. P.; Freed, J. H. Multiple-Quantum ESR and Distance Measurements. *Chem. Phys. Lett.* **1999,** *313*, 145-154, https://doi.org/10.1016/S0009-2614(99)00972-0.

(45) Gamble Jarvi, A.; Cunningham, T. F.; Saxena, S. Efficient Localization of a Native Metal Ion within a Protein by Cu^{2+}-Based EPR Distance Measurements. *Phys. Chem. Chem. Phys.* **2019,** *21*, 10238-10243, https://doi.org/10.1039/C8CP07143H.

(46) Gamble Jarvi, A.; Ranguelova, K.; Ghosh, S.; Weber, R. T.; Saxena, S. On the Use of Q-Band Double Electron–Electron Resonance To Resolve the Relative Orientations of Two Double Histidine-Bound Cu^{2+} Ions in a Protein. *J. Phys. Chem. B* **2018,** *122*, 10669-10677, https://doi.org/10.1021/acs.jpcb.8b07727.

(47) Giannoulis, A.; Yang, Y.; Gong, Y.-J.; Tan, X.; Feintuch, A.; Carmieli, R.; Bahrenberg, T.; Liu, Y.; Su, X.-C.; Goldfarb, D. DEER Distance Measurements on Trityl/Trityl and Gd(III)/Trityl Labelled Proteins. *Phys. Chem. Chem. Phys.* **2019,** *21*, 10217-10227, https://doi.org/10.1039/C8CP07249C.

(48) Wort, J. L.; Ackermann, K.; Norman, D. G.; Bode, B. E. A General Model to Optimise Cu^{II} Labelling Efficiency of Double-Histidine Motifs for Pulse Dipolar EPR Applications. *Phys. Chem. Chem. Phys.* **2021,** *23*, 3810-3819, https://doi.org/10.1039/D0CP06196D.

(49) Polyhach, Y.; Bordignon, E.; Tschaggelar, R.; Gandra, S.; Godt, A.; Jeschke, G. High Sensitivity and Versatility of the DEER Experiment on Nitroxide Radical Pairs at Q-Band Frequencies. *Phys. Chem. Chem. Phys.* **2012,** *14*, 10762-10773, https://doi.org/10.1039/C2CP41520H.

(50) Ackermann, K.; Giannoulis, A.; Cordes, D. B.; Slawin, A. M. Z.; Bode, B. E. Assessing Dimerisation Degree and Cooperativity in a Biomimetic Small-Molecule Model by Pulsed EPR. *Chem. Commun.* **2015,** *51*, 5257-5260, https://doi.org/10.1039/C4CC08656B.

(51) Bode, B. E.; Margraf, D.; Plackmeyer, J.; Dürner, G.; Prisner, T. F.; Schiemann, O. Counting the Monomers in Nanometer-Sized Oligomers by Pulsed Electron−Electron Double Resonance. *J. Am. Chem. Soc.* **2007,** *129*, 6736-6745, https://doi.org/10.1021/ja065787t.

(52) Giannoulis, A.; Ackermann, K.; Spindler, P. E.; Higgins, C.; Cordes, D. B.; Slawin, A. M. Z.; Prisner, T. F.; Bode, B. E. Nitroxide–Nitroxide and Nitroxide–Metal Distance Measurements in Transition Metal Complexes with Two or Three Paramagnetic Centres Give Access to Thermodynamic and Kinetic Stabilities. *Phys. Chem. Chem. Phys.* **2018,** *20*, 11196-11205, https://doi.org/10.1039/C8CP01611A.

(53) Giannoulis, A.; Oranges, M.; Bode, B. E. Monitoring Complex Formation by Relaxation-Induced Pulse Electron Paramagnetic Resonance Distance Measurements. *ChemPhysChem* **2017,** *18*, 2318-2321, https://doi.org/10.1002/cphc.201700666.

(54) Merz, G. E.; Borbat, P. P.; Muok, A. R.; Srivastava, M.; Bunck, D. N.; Freed, J. H.; Crane, B. R. Site-Specific Incorporation of a Cu^{2+} Spin Label into Proteins for Measuring Distances by Pulsed Dipolar Electron Spin Resonance Spectroscopy. *J. Phys. Chem. B* **2018,** *122*, 9443-9451, https://doi.org/10.1021/acs.jpcb.8b05619.

(55) Jeschke, G., Interpretation of Dipolar EPR Data in Terms of Protein Structure. In *Structural Information from Spin-Labels and Intrinsic Paramagnetic Centres in the Biosciences*, Timmel, C. R.; Harmer, J. R., Eds. Springer Berlin Heidelberg: Berlin, Heidelberg, 2013; pp 83-120.

(56) Jeschke, G. DEER Distance Measurements on Proteins. *Annu. Rev. Phys. Chem.* **2012,** *63*, 419-446, https://doi.org/10.1146/annurev-physchem-032511-143716.

(57) Ward, R.; Bowman, A.; Sozudogru, E.; El-Mkami, H.; Owen-Hughes, T.; Norman, D. G. EPR Distance Measurements in Deuterated Proteins. *J. Magn. Reson.* **2010,** *207*, 164-167, https://doi.org/10.1016/j.jmr.2010.08.002.

(58) Šimėnas, M.; O'Sullivan, J.; Zollitsch, C. W.; Kennedy, O.; Seif-Eddine, M.; Ritsch, I.; Hülsmann, M.; Qi, M.; Godt, A.; Roessler, M. M.; Jeschke, G.; Morton, J. J. L. A Sensitivity Leap for X-Band EPR Using a Probehead with a Cryogenic Preamplifier. *J. Magn. Reson.* **2021,** *322*, 106876, https://doi.org/10.1016/j.jmr.2020.106876.